I R A M P
4(1), June 2013, pp. 23-28

ISSN: 2229-3159

Measurement of Hydrogen Balmer Series Lines Following Laser-inducedoptical Breakdown in Laboratory Air

LAUREN D. SWAFFORD[1] AND CHRISTIAN G. PARIGGER[1,a]

[1]*University of Tennessee Space Institute, Center for Laser Applications, Tullahoma, TN 37388, USA*
E-mail: cparigge@tennessee.edu

ABSTRACT: Emission profiles for the Balmer series hydrogen alpha and beta lines are measured following laser-induced optical breakdown. The spatial and temporal evolution of the hydrogen alpha and beta spectra is explored using a typical laser-induced breakdown spectroscopy (LIBS) experimental arrangement. A Q-switched Nd: YAG laser, operated at a wavelength of 1064 nm, is focused to generate a micro-plasma in laboratory air. The atomic hydrogen Balmer series lines are used to infer electron density by measuring the Stark broadened line profile and comparing the results with previous measurements in pure hydrogen gas.

PAC Snumbers: 32.70.Jz,33.70.Jg,52.50.Jm,78.47.dc,82.80.-d,95.55Qf,95.75.Fg.

Keywords: Spectral lineshapesand shifts, laser-induced breakdown spectroscopy, time-resolved spectroscopy, laser-induced breakdown, spectroscopy in astronomy.

I. INTRODUCTION

Laser-induced breakdown spectroscopy (LIBS) has been a useful tool for exploring species densities such as electron density of micro-plasma from a measured full width half maximum spectral line values [1,2]. In this brief research study, we have taken specific note of the hydrogen Balmer series alpha and beta lines for the purpose of determining their temporal and spatial evolution. For laser-induced optical breakdown in laboratory air, the hydrogen alpha line does not begin to appear until typically 0.4 μs after the breakdown event induced by the short, 13 ns pulse-width Nd:YAG laser radiation. The beta line emerges around 1.6 μs after initiation of optical breakdown. By measuring the full width half max (FWHM) of the Stark-broadened hydrogen lines the transient characteristics of the micro-plasma are examined [3-5]. Analysis of the generated micro-plasma is performed to deduce electron density and to a certain degree, temperature as well. The FWHM can be reasonably measured and compared with Stark Broadening Tables (SBT) from Griem [6] and Oks [7], using various theories in determining electron density as also recently discussed by Pardini *et al.* [8]. We are able to accurately explore transient phenomena subsequent to decay of free electron radiation. The experimental procedures for measurement of micro-plasma spectroscopic 'fingerprints' include wavelength calibration, background correction, and most importantly, sensitivity correction of the detector.

II. EXPERIMENTAL DETAILS

A typical laser-induced breakdown arrangement is employed for our studies and for data collection. A DCR-2A Quanta-Ray Nd:YAG laser with a 13 ns, 190 mJ/pulse beam, operating at a fundamental wavelength of 1064 nm and frequency doubled 532 nm, is passed through a beam splitter for the purpose of deflecting 532 nm frequency to a beam dump, as can be seen in Figure 1, allowing the 1064 nm wavelength light to pass through. The laser is triggered at 10 Hz, commensurate with the 50 Hz optical multichannel analyzer OMA readout. The 1064 nm radiation is focused to a spot size on the order of 50 μm, causing breakdown in laboratory air. The radiation from the

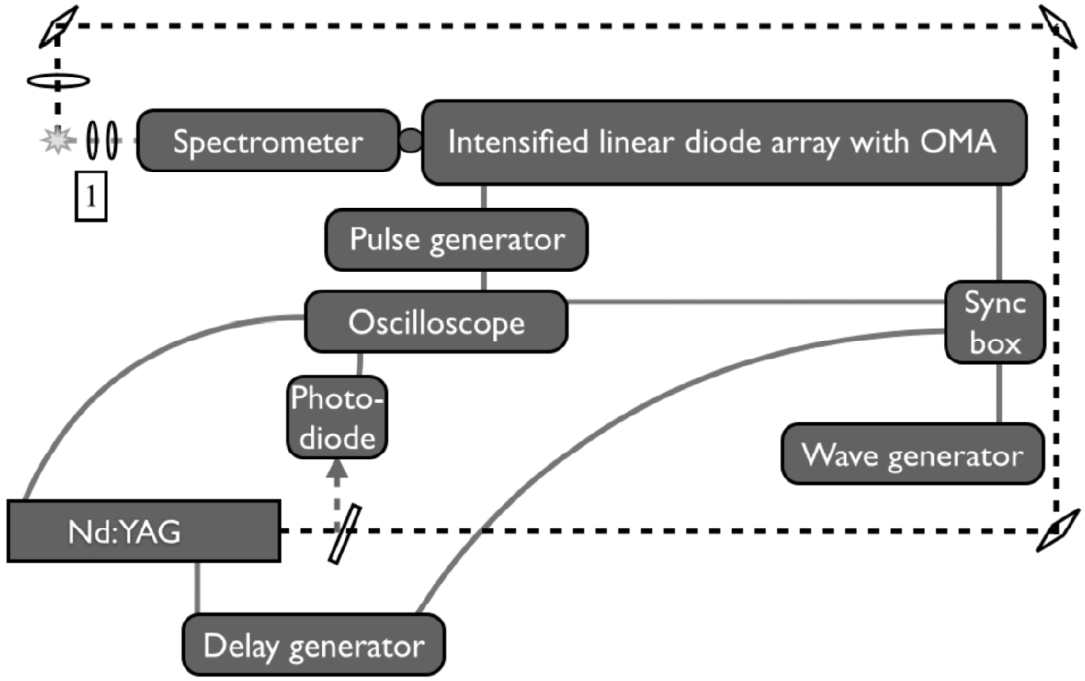

Figure 1: Schematic Diagram for LIBS measurements. Laser-induced optical breakdown is generated in laboratory air, and the micro-plasma is imaged onto the entrance slit of the spectrometer (see box labeled 1).

breakdown event is imaged onto the spectrometer slit. The pulse energy for the initial laser beam is 75 mJ. The generated micro-plasma is dispersed by the HR6400 .6m Jobin-Yvon spectrometer.

The spectra are collected with an intensified linear diode array and OMA. We use an 1800 grooves/mm grating to disperse the emitted plasma radiation. A delay generator (Stanford model DG535) was used to trigger the OMA. A gate width of 0.05 μs was selected and a time delay ranging from 0.2 to 1.0 μs was utilized for hydrogen alpha line measurements. For a detailed characterization of the hydrogen alpha line's temporal evolution, data was captured in 0.1μs increments for the delay time. The brevity of a 0.05 μs gate allowed us to focus on a specific temporal window for the measurements.

III. ANALYSIS

The recorded data were post-processed following the procedures discussed below. Successful time-resolved spectroscopy requires various calibration procedures. Initially, the data from the spectrometer was extracted into a wavelength vs. intensity text file. The file then had to be background subtracted using a background file that was collected at the same gate width as our data, which was achieved in excel. For the wavelength calibration a hydrogen lamp was used to calibrate the OMA. Lastly, a 'Python' calibration program [9] was used for the sensitivity calibration. The program applied a least square fit and interpolated the data file, calibration file, and ideal blackbody curve. The calibration file was collected by using a tungsten lamp to create a black body calibration spectrum for our spectrometer-detector arrangement. Using a pyrometer, the temperature of the calibration lamp was recorded to be 2910 K.

Collecting data at various times after the event allows us to observe the plasma evolution. Laboratory air species such as nitrogen and oxygen cause an increase number of electrons in the micro-plasma, therefore, the hydrogen alpha and beta lines emerge time-delayed after the optical breakdown event. The temporal evolution of the hydrogen lines are of particular interest. The hydrogen alpha line does not appear until 0.3 to 0.4 μs after the generation of plasma. Figures 2 and 3 illustrate this behavior. For this reason some of the non-hydrogen data was masked at very early delay times in order to fit a reasonable curve to the alpha line.

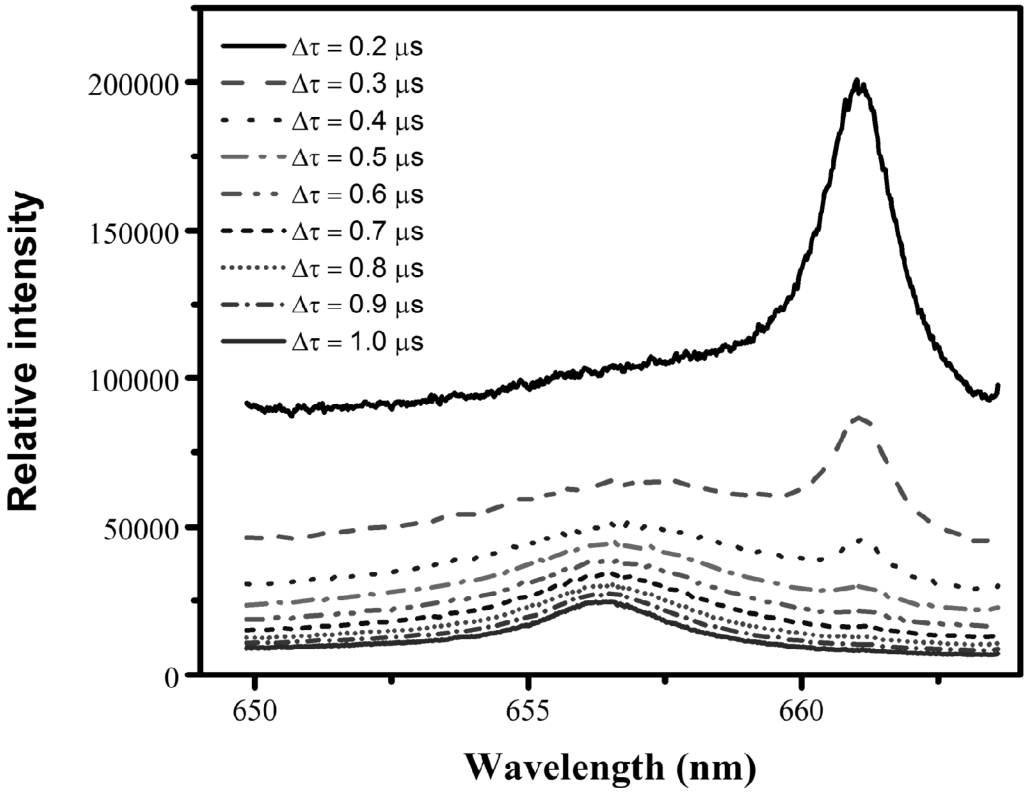

Figure 2: Temporal evolution of plasma emissions from 0.2 μs to 1.0 μs after optical breakdown.

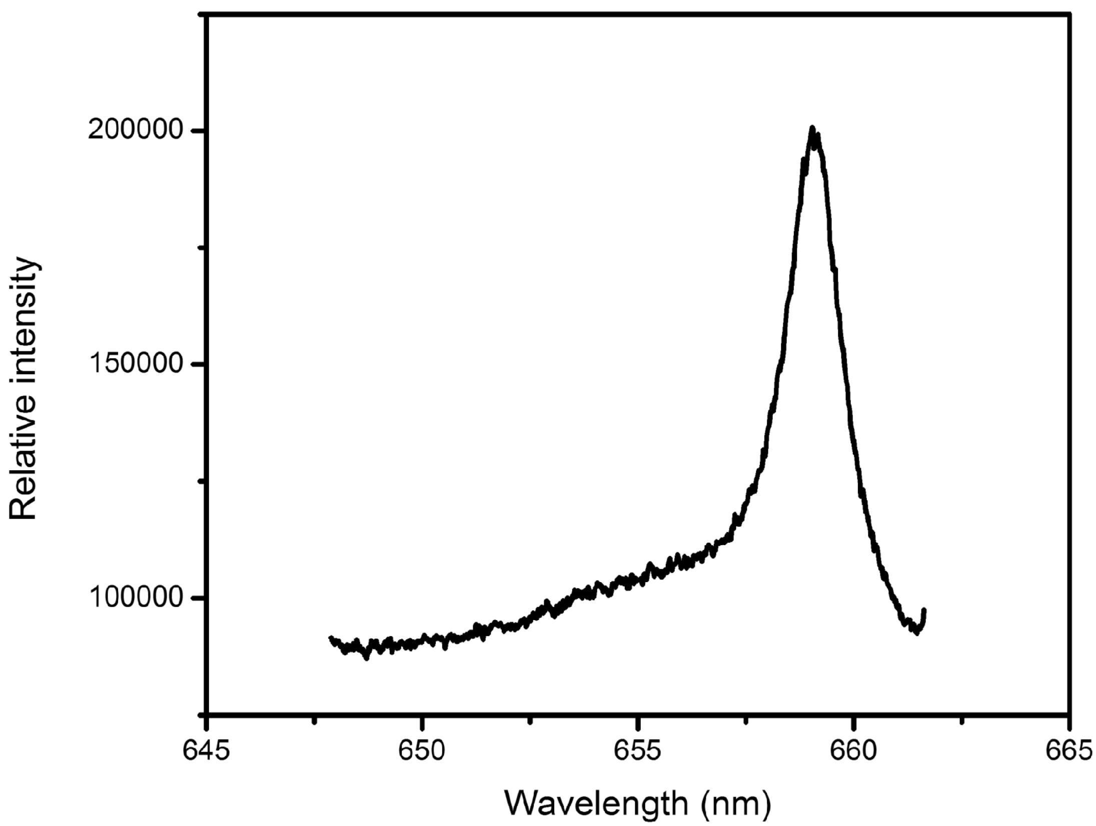

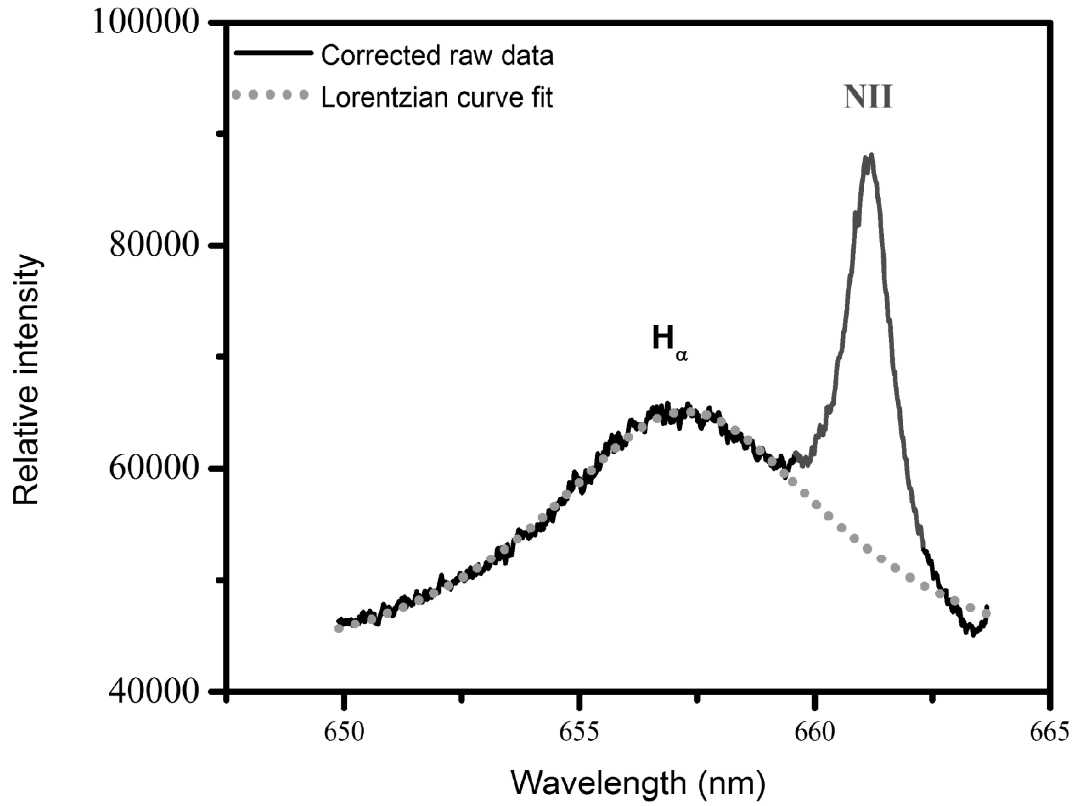

Figure 3: Micro-plasma emissions for 0.2 μs (above) and 0.3 μs (below) time delay. Hydrogen alpha appears to become discernible for 0.3 μs time delay.

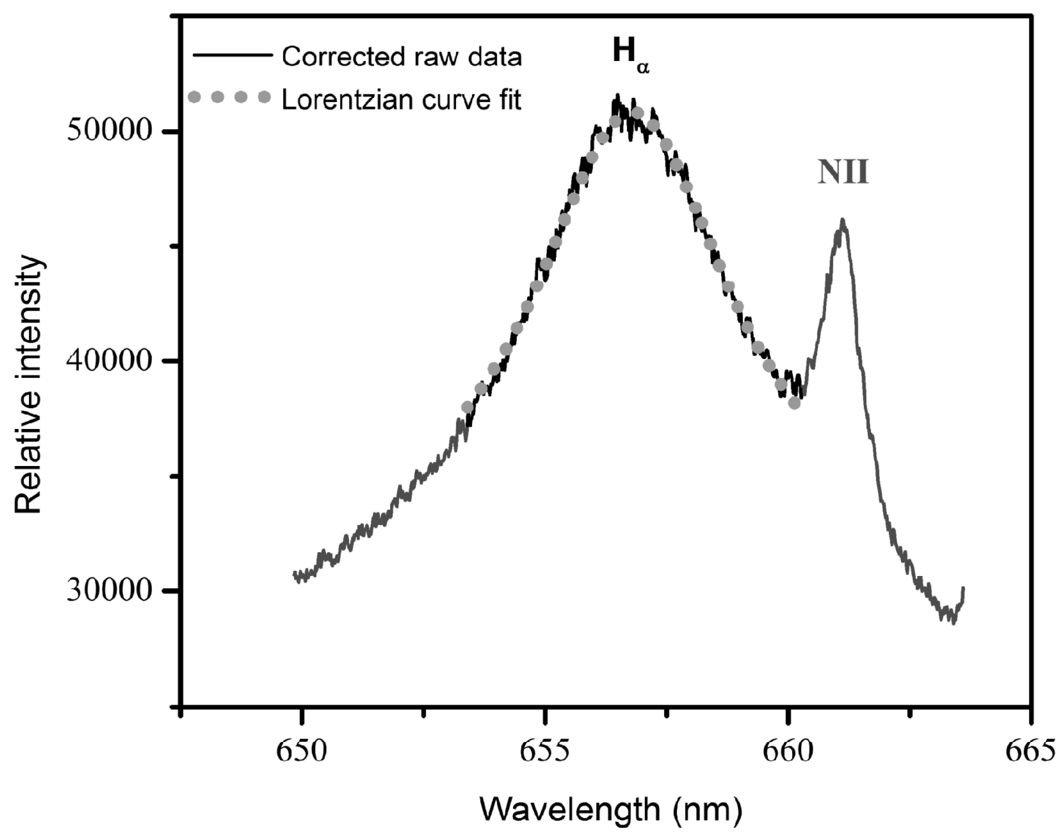

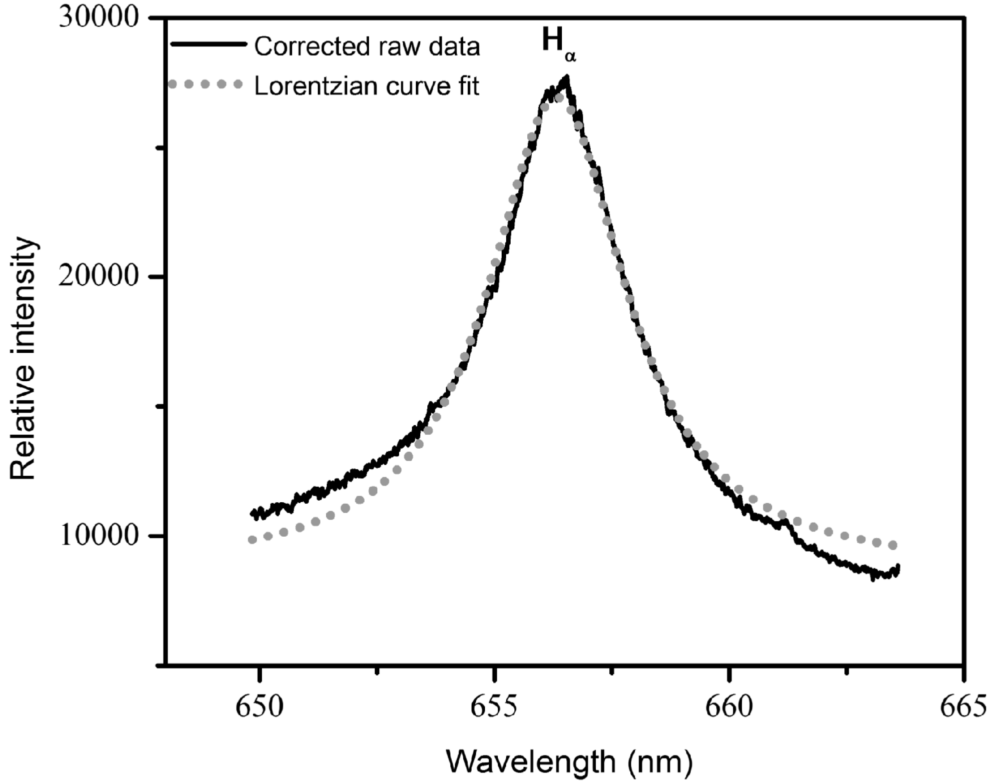

Figure 4: Hydrogen alpha at a time delay of 0.4 μs (above) and 1.0 μs (below). At 0.4 μs time delay, the hydrogen alpha line is well-developed despite free-electron background and presence of species such as oxygen and nitrogen in laboratory air.

A Lorentzian curve fit was performed using 'Originlab' software, and the full width half maximum (FWHM) and redshift are extracted from the curve fits. Once calibrated and sensitivity-corrected, the FWHM of the line profiles can be determined. The results are subsequently compared to Stark broadening tables as documented in, for example, Refs. [3,4]. Using the equation $N_e[m^{-3}] = 10^{23}\times(w_{SA}[nm]/1.098)^{1.47135}$ from Konjević *et al.* [10], the electron density can be inferred. Here, $N_e[m^{-3}]$ is the electron density and $w_{SA}[nm]$ is the Stark full-width-half-area [10]. The formula for hydrogen beta is similar to that of the hydrogen alpha line, $N_e[m^{-3}]=10^{22}\times(w_S[nm]/4.8)^{1.46808}$. Here, w_S is the Stark width [10].

The calculation of the Stark full-width-half-area is not practical for determining electron density through plasma diagnostics. Fortunately, the hydrogen alpha line-shape is fit well by a Lorentzian function. One can approximate that $w_{SA} = w_S = w_L$, where w_L is the Lorentzian FWHM. Figure 4 illustrates results from Lorentzian curve fitting. Tables 1-2 summarize the results for measured FWHM, including inferences for electron density, and red-shifts as well. Figures 5-6 illustrate recorded hydrogen beta line profiles.

Table 1
Hydrogen alpha FWHM, electron density (left) and red shift (right) from 0.3 to 1.0 μs.

time delay (μs)	*FWHM (nm)*	*density × $10^{23}(m^{-3})$*	*time delay (μs)*	*red shift (nm)*
0.3	7.808 ± 0.105	18.0	0.3	0.984
0.4	6.415 ± 0.064	13.5	0.4	0.559
0.5	5.469 ± 0.041	9.0	0.5	0.335
0.6	4.791 ± 0.039	8.8	0.6	0.202
0.7	4.348 ± 0.037	6.4	0.7	0.155
0.8	3.940 ± 0.035	6.6	0.8	0.081
0.9	3.596 ± 0.035	5.7	0.9	0.048
1.0	3.306 ± 0.034	5.1	1.0	0.019

The hydrogen beta line was also measured in laboratory air breakdown, and much like the hydrogen alpha lines, could not be seen immediately due to free-electron background and the presence of oxygen and nitrogen in the air. The hydrogen beta line begins to emerge from the spectrum at time delays longer than 1.6 μs. Table 2 shows measured FWHM and inferred electron density.

Table 2
Measured FWHM and electron density inferred from the hydrogen beta line.

delay time(μs)	*FWHM(nm)*	*Density×10^{23}(m^{-3})*
5.0	4.039 ± 0.079	0.776
6.0	3.380 ± 0.055	0.598
7.0	2.896 ± 0.043	0.476
8.0	2.506 ± 0.037	0.385
9.0	2.186 ± 0.032	0.315
10.0	1.899 ± 0.043	0.256

The indicated uncertainties in the full-width-half-maximum tables are due to error margins in fitting, yet the actual sigma error is estimated to be up to an order of magnitude larger, for example, due to difficulties in determining the baselines early in the plasma decay. The measurements for the hydrogen alpha line at the time delay of 0.3 μs also shows a slightly larger margin of error than other measurements at later time delays because the oxygen and

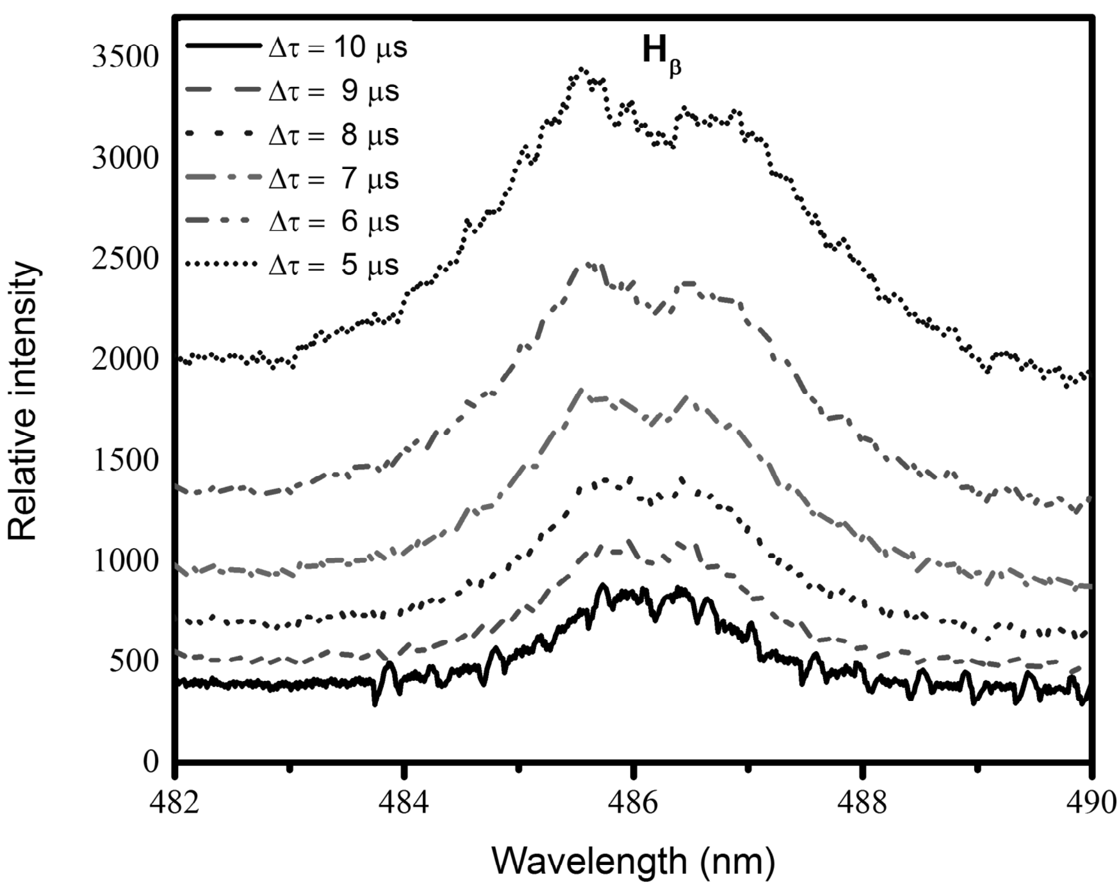

Figure 5: Temporal evolution of the hydrogen beta line. The individual line profiles represent single shot data records.

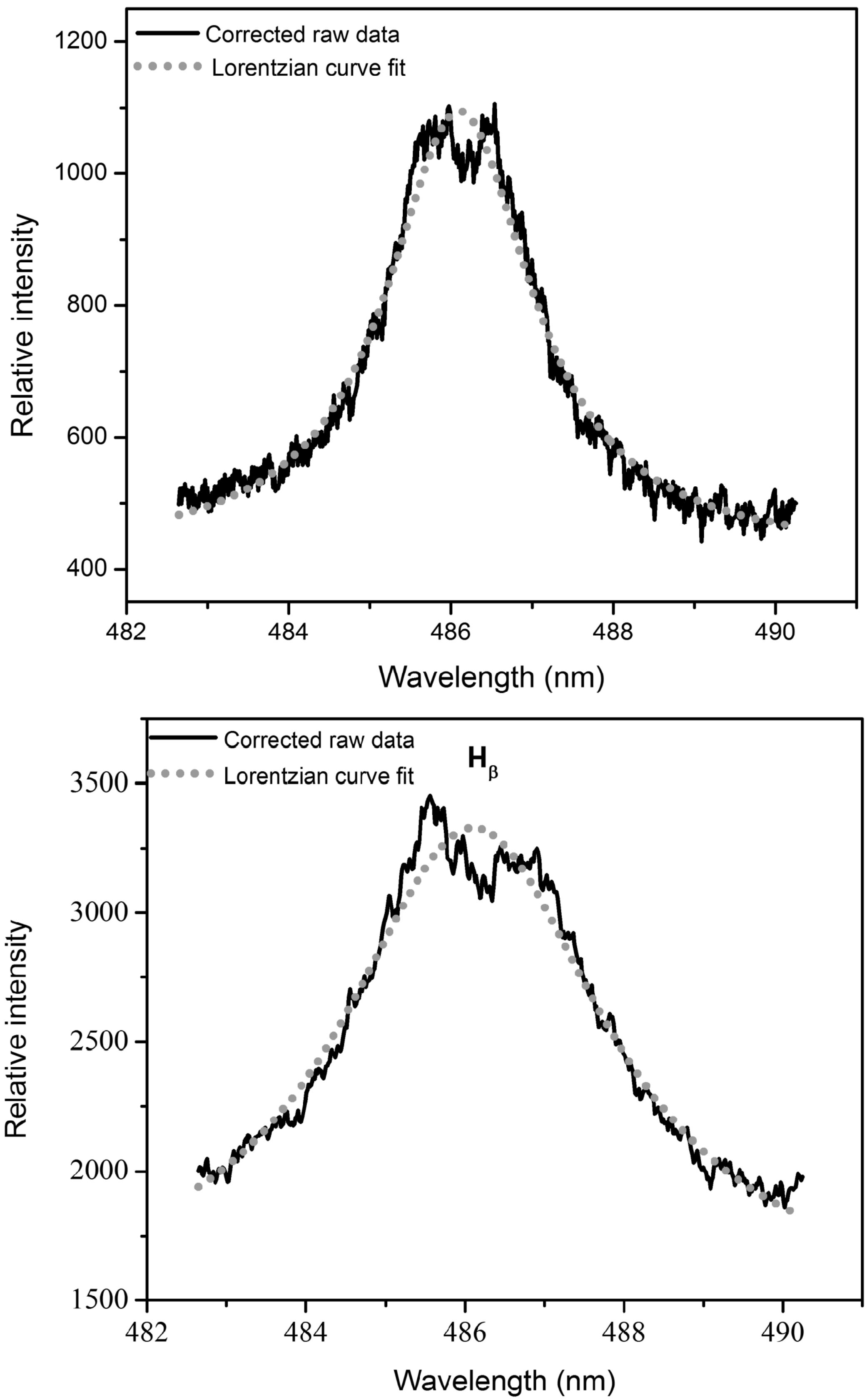

Figure 6: Hydrogen beta line fitted with a Lorentzian curve at 6.0 µs (above) and 9.0 µs (below) time delay after optical breakdown.

nitrogen still mask a significant portion of the curve. Fitting of the hydrogen beta line with Lorentzian profiles is less precise than that of the hydrogen alpha line because the peak of the line shape is inconsistent with the Lorentzian function with which it has been fit. Having taken that note, the experimental values calculated in this paper are consistent with those found in Parigger *et al.* [3], Pardini *et al.*[8], and Konjević *et al.* [10]. In future analysis of these lines we suggest to explore the self-absorption properties of the hydrogen lines due to radiative transfer of line radiation through the micro-plasma with the expectation of seeing a decrease in line width and an increase in relative intensity [10]. Equally, for future experiments, measurements of spatially resolved line profiles are indicated to map the spatial plasma evolution along with the temporal evolution presented in this work on laser-induced plasma in laboratory air.

IV. CONCLUSIONS

Time-resolved analysis of laser induced optical breakdown in laboratory air has been used to measure the full width at half maximum of the hydrogen alpha and beta Balmer series lines. From the FWHM electron number density of the hydrogen alpha line was found to have a range of 16×10^{23} electrons/m^3 at 0.3 μs and 4.8×10^{23} electrons/m^3 at 1.0 μs time delay.

Acknowledgements

LDS and CGP thank for support in part by The Center for Laser Applications at The University of Tennessee Space Institute.

References

[1] A.W. Miziolek., V. Palleschi, I. Schechter eds., Laser Induced Breakdown Spectroscopy. Cambridge University Press, New York, (2006).

[2] D. A. Cremers and L. J. Radziemski, *Handbook of laser-induced Breakdown Spectroscopy*. John Wiley, New York, (2006).

[3] C.G. Parigger, D. H. Plemmons, E. Oks, *Appl. Op*. 42, 5992 (2003).

[4] N. Konjeviæ, A. Lesage, J. R. Fuhr and W. L. Wiese, *J. Phys. Chem. Ref. Data* **31**, 819, (2002).

[5] C. G. Parigger, M. Dackman, and J. O. Hornkohl, *Appl. Opt*. **47**, G1, (2008).

[6] H.R. Griem, *Spectral Line Broadening by Plasmas.* Academic Press, New York, (1974).

[7] E. Oks, *Stark broadening of hydrogen and hydrogen-like spectral lines in plasmas: the physical insight*. Alpha Science Int., Oxford, (2006).

[8] L. Pardini, S. Legnaioli, G. Lorenzetti, V. Palleschi, R. Gaudiuso, D.M. Diaz Pace, F. Anabitarte Garcia, G. de Holanda Cavalcanti, and C. Parigger, Spectrochim. Acta B, in press, *http://dx.doi.org/10.1016/j.sab.2013.05.030 (2013).*

[9] Private communication, Alexander C. Woods (2012).

[10] N. Konjević, M. Ivkoviæ, N. Sakan, Spectrochim. Acta B, **76**, 16, (2012).